Theory of electron capture from a hydrogenlike ion by a bare ion: Intermediate-state contributions to the amplitude

Steven Alston
Behlen Laboratory of Physics, University of Nebraska-Lincoln, Lincoln, Nebraska 68588
(Received 10 June 1982)

Electron capture from a hydrogenlike ion of large nuclear charge $Z_T e$ by a bare ion of charge $Z_P e$ moving with speed v has been studied using the strong-potential Born approximation to the amplitude. Under the conditions $Z_P \ll Z_T$ and $Z_P e^2 \ll \hbar v$, it is shown that, in comparison with the impulse approximation, the correct weighting of the target spectrum of intermediate states in the strong-potential Born theory significantly alters the $1s \rightarrow 1s$ cross section and at the same time makes peaking approximations to the amplitude more realistic, even for low v. The specific cases of $Z_T = 6$, 10, and 18 are treated over the velocity range $Z_T/3 \lesssim \hbar v/e^2 \lesssim Z_T/(0.3)$. Instituting a one-electron model, K-shell capture cross sections and probabilities for protons on carbon, neon, and argon are calculated and compared with experiment. The strong-potential Born theory is seen to give a good representation of the data. Total cross sections for $1s \rightarrow 1s$ capture for $Z_P = Z_T = 1$ are also presented.

I. INTRODUCTION

Although the study of electron capture in ion-atom collisions dates from the early days of quantum mechanics,[1,2] a unified treatment covering a wide range of energies has not yet emerged. Only more limited results exist, for example, in nearly symmetric collisions when a molecular picture is adequate[3] at low velocities or a two-state approximation is valid at velocities close to the initial orbital velocity,[4] and at asymptotically high velocities when a double-scattering mechanism dominates.[5] In the past few years, however, a promising framework has evolved for inner-shell capture by a light bare ion in which the incident velocity v is much larger than the mean orbital velocity of the final bound state. This framework, which is capable of treating the intermediate and high-velocity regions, has been developed by Briggs,[6] Macek and co-workers,[7–9] and others.[10]

We can readily grasp the novel features of the framework in terms of an electronic energy level diagram.[9] Because the independent-electron approximation can be reasonably applied to the inner shells of atoms, we consider capture from a hydrogenlike ion of nuclear charge $Z_T e$ by a bare ion of charge $Z_P e$ incident with velocity v and for which Z_P is much less than Z_T. Initially, the electron is bound in the ground state of the target with energy ϵ_i, but through capture it acquires the bound-state energy ϵ_f and the kinetic energy $\frac{1}{2}mv^2$, with m the electron mass. If we plot the energy spectrum of the target in the diagram of Fig. 1, then, since the final bound electron-projectile system moves with velocity v relative to the almost stationary target ion, we can place the projectile spectrum on the same diagram shifted upwards from the target threshold by an amount $\frac{1}{2}mv^2$. Figure 1 is plotted to scale for $Z_T = 4$ and $Z_P = 1$. The very small extent of the projectile spectrum as compared to that of the target is readily apparent from the figure.

We describe the capture process as a two-step re-

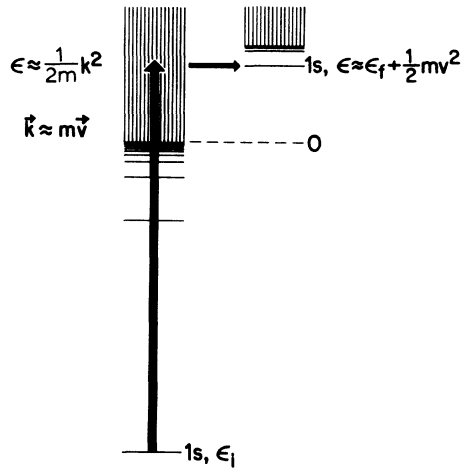

FIG. 1. Electronic energy-level diagram showing the two-step picture of capture: (1) virtual ionization and (2) attachment. The target spectrum appears on the left and the final-state projectile spectrum on the right. The figure is plotted to scale for $Z_P = 1$, $Z_T = 4$.

action in which the electron is virtually ionized in the field of the target and then becomes attached to the projectile ion. Ionization provides the necessary means for the electron gaining the kinetic energy $\frac{1}{2}mv^2$ and momentum $m\vec{v}$ of the final state. The novel aspect of the present formulation is the use of target states centered around the most favorable energy $\frac{1}{2}mv^2+\epsilon_f$ to mediate the capture reaction. Such states have momentum of the order of $m\vec{v}$. The lower target spectrum is, moreover, seen to play a significant role when the velocity decreases.

Because capture goes via intermediate states of the stronger target potential and since the theory is of the Born type, it is termed the strong-potential Born (SPB) theory; it is unique among second Born-approximation—type theories. The plane-wave second Born-approximation theory,[11] continuum intermediate state,[12] and eikonal[13] theories do not contain the target bound states at all and approximate the continuum states in various ways. The impulse approximation[6] does contain the lower target states but in an incorrect manner; for example, the bound states have exponentially increasing wave functions. None of these theories is applicable from an *a priori* standpoint in the velocity range $Z_P \ll v \lesssim Z_T$ with v in atomic units. No such restriction exists for the strong-potential Born theory and yet it also agrees with the third Born-approximation theory at asymptotically high velocities.[9,14] The SPB amplitude is the only one containing the weaker electron-projectile potential consistently to lowest order.[9] We conclude that the SPB theory offers a comprehensive approach to inner-shell capture for intermediate to high impact velocities.[15]

The purpose of this paper is to explore the importance of the target spectrum to the capture amplitude as a function of the impact velocity v and charge asymmetry. We do this by contrasting the correct weighting of the virtual states in the SPB approximation with the inconsistent weighting in the impulse-approximation (IA) theory. We further present total cross sections and probabilities for K-shell capture by protons from carbon, neon, and argon and compare with experiment. The SPB values give generally good agreement with the data, particularly as the asymmetry increases. Our results are restricted to $1s \rightarrow 1s$ captures, but the formalism is developed more generally.

The recent interest[8–10,16–18] in the theory of inner-shell capture started with Briggs's use[6] of the impulse approximation in asymmetric collisions. He realized that the IA results from keeping the lowest term of an expansion of the full Green's operator in the natural parameter Z_P/Z_T. Subsequent calculations include those of Jakubassa-Amundsen and Amundsen[10,16] and Kocbach.[17] These studies, covering a moderate range of charge asymmetry, show that cross sections obtained using a peaking approximation differ considerably from exact ones with the discrepancies increasing as the asymmetry decreases, especially in the intermediate velocity region. For example, at a velocity $v=\frac{1}{2}Z_T$, the exact IA value for the $1s \rightarrow 1s$ total cross section differs from the peaking approximation value[6,9,10] by $\sim 30\%$ for protons on argon ($Z_T=18$) and by $\sim 50\%$ for protons on neon ($Z_T=10$) even though the expansion parameter $(Z_P/v)^2$ of the peaking approximation equals 0.01 and 0.04, respectively, for the two cases.

Macek and Taulbjerg have shown,[8] however, that the impulse approximation is derived inconsistently by neglecting certain off-energy-shell terms of order $(Z_T/v)^2$ which become large for v below Z_T. The strong-potential Born theory corrects this problem so that only errors of the order $(Z_P/v)^2$ remain even for low v less than Z_T but much greater than Z_P. We further argue here, following the comments of Macek and Alston,[9] that the SPB amplitude has inherently better peaking qualities as a result of the modified weighting of the intermediate states as compared to the IA. This in turn implies that an evaluation of the SPB amplitude using a less restrictive peaking approximation produces only relatively small changes in the cross sections. Our study maps the corrections as v and Z_T vary holding Z_P constant and interprets the corrections in terms of the relative importance of the upper bound state and lower continuum spectrum of the target. Since we directly compare the SPB and IA cross sections and because a variety of inner-shell models are used in the literature, we present SPB and IA calculations using identical models and identical approximations.

The impulse approximation and strong potential Born amplitudes for capture into the ground state can be reduced to three-dimensional integrals of the form

$$A=\int d^3p\, f(\vec{p})(p^2+Z_P^2)^{-\gamma(\vec{p})},$$

in which γ may be a complex function of $\vec{p}$ with real part greater than or equal to 2. On account of the conditions $Z_P/v \ll 1$ and $Z_P/Z_T \ll 1$ assumed in the present treatment, the dominant contributions to this integral arise from the region near the origin where the integrand as a whole is peaked and where f and γ vary slowly. We can consequently simplify the integrand by neglecting part or all of the $\vec{p}$ dependence of f and γ to obtain peaking approximations to A.

Two separate peaking approximations are employed here. In one of these, which we call full peaking (FP), all of the $\vec{p}$ dependence of f and γ is

neglected; the amplitude is

$$A^{\mathrm{FP}} \approx f(0) \int d^3p (p^2+Z_P^2)^{-\gamma(0)} .$$

The second peaking approximation is less restrictive and more complicated. Since f is more peaked for $\vec{p}$ transverse to the projectile direction $\vec{v}$ than for $\vec{p}$ parallel to it and since γ can be expressed as a function of p_z only, we introduce the transverse peaking (TP) approximation[10] in which we neglect only the $\vec{p}_\perp$ components of $\vec{p}$ in f; the amplitude is

$$A^{\mathrm{TP}} \approx \int dp_z f(p_z\hat{v}) \int d^2p_\perp (p^2+Z_P^2)^{-\gamma(p_z\hat{v})} .$$

It will be seen that an important distinguishing feature of A^{TP} is a more accurate representation of the target spectrum near the ionization limit. The IA amplitude in both the FP and TP approximations is obtained in analytic form thus allowing a determination of which parts of the amplitude change significantly between approximations.

We evaluate the p_z integral in the transversely peaked SPB amplitude by closing the integration contour in the upper half-plane. This is necessitated by the close proximity of the bound-state poles to the real p_z axis. An exact evaluation of the SPB amplitude would not alter the situation. Thus, the method adopted here for calculating the amplitude proceeds along the same lines as that needed for an exact evaluation.

Jakubassa-Amundsen and Amundsen[18] have also performed improved SPB calculations but the level of approximation used is not entirely clear. They did not attempt a systematic determination of the effects of the off-shell term and its connection with the target spectrum. When $v \gtrsim Z_T$, both the SPB and IA cross sections obtained using the transverse peaking approximation should converge to the full peaking cross sections as v increases, until very high v where the Thomas peak[5] dominates and the deviations may increase again (although their magnitudes are small). This implies that the ratio of the corresponding Jakubassa-Amundsen and Amundsen cross sections should converge, within a factor of the order of Z_P/Z_T, to the Macek and Taulbjerg[8] factor

$$|M_1(\nu)|^2 = 2/[(1+\nu^2)(1+e^{-2\pi\nu})] ,$$

where $\nu = Z_T/v$. Their cross sections do not exhibit this behavior until relativistic velocities are reached. Our cross sections do converge in the expected manner. At the lower limit of the velocity region treated $v \approx Z_T/3$ we do find better agreement with the Jakubassa-Amundsen and Amundsen TP-FP deviations.

The plan of the paper is as follows. Section II A sketches the derivation of the SPB amplitude to a form where the transverse and full peaking approximations can be introduced. We carry through these approximations in Sec. II B. A model potential is introduced and cross-section formulas outlined in Sec. II C. Comparison of the SPB and IA cross sections for hydrogenlike targets is undertaken in Sec. III A. Model potential calculations are compared with experiment in Sec. III B. Section III C contains results for $Z_P = Z_T = 1$. In Appendix A, we estimate the contributions to the amplitude arising from the region of intermediate momenta surrounding the singularity of the electron-projectile interaction in momentum space. Appendix B gives a justification for evaluating the transverse peaking amplitudes by closing the p_z integration contour in the upper half-plane.

Much of the development of Sec. II A relies on Secs. II and IV of Macek and Alston.[9] The prior form of the capture amplitude is used and atomic units ($\hbar = m = e = 1$) are assumed. In general, the coordinate and momentum representations are related by the equation

$$\phi(\vec{r}) = (2\pi)^{-3/2} \int d^3p \, \tilde{\phi}(\vec{p}) e^{i\vec{p}\cdot\vec{r}} .$$

The norm $|\vec{q}|$ of a vector $\vec{q}$ is simply denoted q. With $\vec{v}$ the impact velocity, we use the notation $q_z\hat{v}$, $\vec{q}_\perp$, respectively, for the components of $\vec{q}$ parallel to and perpendicular to $\vec{v}$ with $\hat{v}$ a unit vector. A plane wave function is denoted

$$\phi_{\vec{k}}(\vec{r}) = (2\pi)^{-3/2} e^{i\vec{k}\cdot\vec{r}} .$$

II. ANALYSIS

A. The strong-potential Born amplitude

Our model consists of a bare ion of charge Z_P incident on a hydrogenlike ion of nuclear charge Z_T with a velocity $v \gg Z_P$. We consider asymmetric collisions with Z_T much greater than Z_P. The initial bound state ϕ_i of the electron and target $(e+T)$ has energy ϵ_i. After capture takes place, the electron and projectile form a bound system $(e+P)$ in the state ϕ_f with energy ϵ_f. We neglect the internuclear potential and any resultant effects such as projectile deflection following the arguments of Wick.[19]

In the total center-of-mass frame, initially P and $(e+T)$ have relative momentum $\vec{K}_i$ and finally T and $(e+P)$ have relative momentum $\vec{K}_f$. Two "average" momentum transfer vectors are defined by the relations[7]

$$\vec{K} = \beta\vec{K}_f - \vec{K}_i$$

and

$$\vec{J} = \alpha\vec{K}_i - \vec{K}_f$$

which are accurate to order m/M_T and m/M_P. Here, we have m, M_P, and M_T as the electron, projectile, and target masses, respectively, and

$$\alpha = M_T/(m+M_T) ,$$

$$\beta = M_P/(m+M_P) .$$

The vector $\vec{K}_i$ is equal to $v_i\vec{v}$ with

$$v_i = M_P(m+M_T)/(m+M_P+M_T) .$$

For the total system energy we have $K_i^2/2v_i + \epsilon_i$.

Macek and Alston have shown[9] that the SPB approximation to the capture amplitude is given by

$$A_{\mathrm{SPB}} = (2\pi)^{3/2} \int d^3p\, \tilde{\phi}_f^*(\vec{p}) \tilde{V}_{Pe}(\vec{p}-\vec{K}) \langle \psi^-_{\vec{p}+\vec{v},\epsilon}(\vec{r}) \,|\, e^{i(\vec{p}-\vec{K})\cdot\vec{r}} \,|\, \phi_i(\vec{r}) \rangle , \tag{1}$$

where $\tilde{\phi}_f^*(\vec{p})$ is the momentum wave function (complex conjugated) of the final bound state and $\tilde{V}_{Pe}(\vec{p}-\vec{K})$ is the electron-projectile interaction in momentum space.

The intermediate off-energy-shell target continuum wave function $\psi^-_{\vec{k},\epsilon}(\vec{r})$ satisfies the inhomogeneous wave equation

$$(H_C - \epsilon + i\eta)\psi^-_{\vec{k},\epsilon}(\vec{r}) = -(\epsilon - \tfrac{1}{2}k^2)\phi_{\vec{k}}(\vec{r}) \tag{2}$$

with η arbitrarily small and positive and with H_C the Hamiltonian for the Coulomb problem with charge Z_T. In Eq. (1), the off-shell energy of the outgoing electron in the target frame is given by[7]

$$\epsilon = \tfrac{1}{2}v^2 + \vec{v}\cdot\vec{p} + \epsilon_f . \tag{3}$$

The capture amplitude Eq. (1) is an overlap integral between $\tilde{\phi}_f^*(\vec{p})$ and an excitation matrix element including $\tilde{V}_{Pe}(\vec{p}-\vec{K})$. The matrix element represents the virtual ionization of the electron into the target continuum induced by the projectile ion. Owing to the presence of $\tilde{\phi}_f^*(\vec{p})$, intermediate states having momentum $m\vec{v}+\vec{p}$ with $p \lesssim Z_P$ produce the major contributions to the amplitude. Thus, in Eq. (1), we have the mathematical expression of the schematic picture of Fig. 1 with capture being related to ionization.

The matrix element involving the off-shell wave function can be reduced to a one-dimensional parametric integral following Kelsey and Macek.[20] Macek and Alston[9] evaluated this integral and approximated the result by making use of the conditions $p \lesssim Z_P$ and $Z_P \ll v$. The capture amplitude is then taken to be primarily a sum of contributions from the region $\vec{p} \approx 0$. But since $\tilde{V}_{Pe}(\vec{p}-\vec{K})$ is a factor in the $\vec{p}$ integrand peaked around $\vec{p}=\vec{K}$, the question arises as to the magnitude of the contributions to the amplitude from the region $\vec{p} \approx \vec{K}$. It is shown in Appendix A that these contributions are of the order $(Z_P/v)^2$ or $(Z_P/Z_T)^2$ and are therefore negligible.

When terms of the order $(Z_P/v)^2$ are neglected, the SPB amplitude for an initial $1s$ state is given from Macek and Alston's Eq. (4.17) in the form

$$A_{\mathrm{SPB}} = (2\pi)^{3/2} \int d^3p\, \tilde{\phi}_f^*(\vec{p}) e^{\pi\nu/2}\Gamma(1+i\nu)\Delta^{-i\nu} M(\vec{p}) \tag{4a}$$

with

$$M(\vec{p}) = 2Z_P \left[\frac{Z_T}{\pi}\right]^{3/2} \frac{e^{\pi\nu/2}\Gamma(1-i\nu)}{|\vec{p}-\vec{K}|^2} \frac{\partial}{\partial\mu}(\mu^2+J^2)^{-1} \left[\frac{(\mu-iv)^2+K^2+2\vec{p}\cdot(\vec{J}-i\mu\hat{v})}{\mu^2+J^2}\right]^{-i\nu} \tag{5}$$

and

$$\Delta = (p^2+Z_P^2)/4(v^2+2\vec{v}\cdot\vec{p}+i\eta) . \tag{6}$$

The quantity ν is defined by the equation

$$\nu \equiv Z_T/(v^2+2\vec{v}\cdot\vec{p}+i\eta)^{1/2} . \tag{7}$$

We have retained the p^2 term of $\tilde{V}_{\mathrm{Pe}}(\vec{p}-\vec{K})$ because of future considerations.

The comparable IA amplitude is obtained from Eq. (4a) by relating the off-shell function $\psi^-_{\vec{k},\epsilon}(\vec{r})$ to the on-shell function $\psi^-_{\vec{k}}(\vec{r})$ which satisfies the homogeneous version of Eq. (2). Specifically, we have, when[9,21] $\epsilon \approx \frac{1}{2}k^2$,

$$\psi^{-*}_{\vec{k},\epsilon}(\vec{r}) \approx \Delta^{-i\nu} e^{\pi\nu/2}\Gamma(1+i\nu)\psi^{-*}_{\vec{k}}(\vec{r}) , \tag{8}$$

where

$$\Delta \equiv -(k^2+X^2)/4X^2 , \quad i\nu \equiv Z_T/X . \tag{9}$$

Here,

$$X = [-2(\epsilon+i\eta)]^{1/2}$$

with $\mathrm{Re}X > 0$. The impulse approximation does not include the factors multiplying $\psi^-_{\vec{k}}(\vec{r})$ in Eq. (8). A comparison of Eq. (8) and Eq. (4a) thus gives the IA amplitude as

$$A_{\mathrm{IA}} = (2\pi)^{3/2} \int d^3p\, \tilde{\phi}_f^*(\vec{p}) M(\vec{p}) , \tag{4b}$$

where terms of order $(Z_P/v)^2$ have been dropped.

Equations (4) can apparently be derived directly from Eq. (1) by substituting Eq. (8) and performing the well-known integral

$$\langle \psi_{\vec{k}}^{-}(\vec{r}) \mid e^{i\vec{q}\cdot\vec{r}} \mid \phi_i(\vec{r}) \rangle \ .$$

This procedure in no way justifies the statement that $A_{\rm SPB}$ Eq. (4a) is accurate to order $(Z_P/v)^2$; however, Eq. (8) does succinctly relate the SPB and the IA approximations based on the small value of Δ. That is, because Δ is of the order of $(Z_P/v)^2$, the reduction of Eq. (1) to Eq. (4a) follows and implies that errors of order Z_T/v are introduced in the IA amplitude Eq. (4b).

The equivalent impact parameter form of the IA amplitude Eq. (4b) was evaluated exactly by Jakubassa-Amundsen and Amundsen.[10,16] A similar calculation of the SPB amplitude Eq. (4a) is complicated by the additional off-shell factor and is a formidable problem. On the other hand, we can evaluate both amplitudes using the same approximation conditions to determine relative contributions of the upper bound states and lower continuum. We therefore pursue an approximate evaluation of the amplitudes using the transverse peaking approximation and then compare with the full peaking values.

B. Approximate evaluation of the amplitudes

To evaluate the amplitudes Eqs. (4) we use the wave-treatment form of the simplification employed by Jakubassa-Amundsen and Amundsen[10] and by Kocbach.[17] With the use of the relation

$$K^2+2\epsilon_i = J^2+2\epsilon_f$$

and taking into account the μ differentiation, the factor $M(\vec{p})$ is seen to be inversely proportional to $K^4 \mid \vec{K}-\vec{p} \mid^2$; accordingly, $\mid A(K_\perp) \mid$ decreases rapidly as $K_\perp$ increases. Here, $A(K_\perp)$ is either of the two amplitudes $A_{\rm SPB}(K_\perp)$ or $A_{\rm IA}(K_\perp)$ and $K_\perp^2 = K^2 - K_z^2$. In the case of protons incident on argon at 12 MeV, the full peaking approximation where $M(\vec{p}) \equiv M(0)$ and $\nu \equiv Z_T/v$ in Eqs. (4) gives[9]

$$\mid A(K_\perp)/A(0) \mid^2 \approx \tfrac{1}{25}$$

for $K_\perp \approx 2 \mid K_z \mid$ and

$$\mid A(K_\perp)/A(0) \mid^2 \approx \tfrac{1}{90}$$

for $K_\perp = 3 \mid K_z \mid$ for both $A_{\rm IA}(K_\perp)$ and $A_{\rm SPB}(K_\perp)$. Similar behavior exists for the amplitudes even at lower energies. For 3-MeV protons on argon, the corresponding ratios are $\frac{1}{20}$ and $\frac{1}{80}$.

Since our goals are to simplify the $\vec{p}$ integral of the amplitudes and to obtain a less restrictive approximation than the full peaking one, we use the above discussion to write our approximate amplitudes by neglecting terms of the order

$$\mid \vec{p}_\perp \cdot \vec{K}_\perp \mid / \mid K_z \mid^2$$

and

$$p_\perp^2 / \mid K_z \mid^2$$

so that

$$M(\vec{p}) \approx M(p_z \hat{v}) \ .$$

Here, we also assume the condition $p \lesssim Z_P \ll v$ of Sec. II A. This simplification allows the $\vec{p}_\perp$ integral to be evaluated analytically. When the final state is $1s$, Eqs. (4) become

$$A_{\rm SPB}^{\rm TP} = 8(\pi^3 Z_P^5)^{1/2} \int_{-\infty}^{+\infty} dp_z \frac{e^{\pi\nu/2}\Gamma(1+i\nu) M(p_z\hat{v})}{(p_z^2+Z_P^2)^{1+i\nu}(1+i\nu)[4(v^2+2vp_z+i\eta)]^{-i\nu}} \tag{10a}$$

and

$$A_{\rm IA}^{\rm TP} = 8(\pi^3 Z_P^5)^{1/2} \int_{-\infty}^{+\infty} dp_z \frac{M(p_z\hat{v})}{p_z^2+Z_P^2} \ . \tag{10b}$$

The superscript TP denotes transverse peaking as terms involving $\vec{p}_\perp \cdot \vec{K}_\perp$ are neglected. Note also that the final state $1s$ designation is suppressed.

We perform the p_z integrations in Eqs. (10) by closing the integration contours in the upper half-plane. The contour used for the SPB amplitude is shown in Fig. 2. For the IA amplitude, a large semicircle is added. Reasons for closing in the upper half-plane and a discussion of the singularity structure of the integrands in Eqs. (10) are presented in Appendix B.

Using the Cauchy-Goursat theorem and neglecting certain contributions following the discussion in Appendix B, Eq. (10a) is expressed as

$$A_{\rm SPB}^{\rm TP} = -8(\pi^3 Z_P^5)^{1/2} \int_\Gamma dp_z \frac{e^{\pi\nu/2}\Gamma(1+i\nu) M(p_z\hat{v})}{(p_z^2+Z_P^2)^{1+i\nu}(1+i\nu)[4(v^2+2vp_z)]^{-i\nu}} \ , \tag{11a}$$

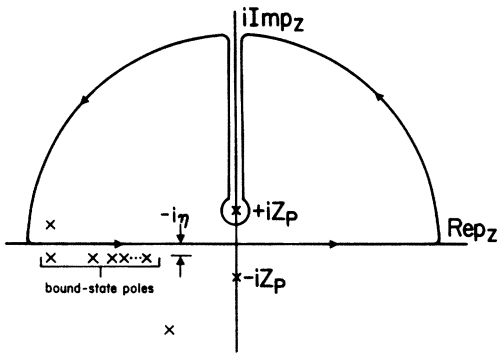

FIG. 2. Closed contour used for the p_z integration in deriving the transverse peaking SPB amplitude Eq. (11a).

where Γ is the contour going around the branch cut taken from $p_z=iZ_P$ to $i\infty$ and where Eqs. (5) and (6) are used. We evaluate Eq. (11a) numerically. From Cauchy's residue theorem, the corresponding IA amplitude is given in the simple form

$$A_{\mathrm{IA}}^{\mathrm{TP}}=8(\pi^5 Z_P^3)^{1/2}M(iZ_P\hat{v}) \tag{11b}$$

with

$$\nu=Z_T/(v+iZ_P)$$

and M defined in Eq. (5).

For comparison purposes, we use the capture amplitudes obtained when $M(\vec{p})=M(0)$ and $\nu=Z_T/v$. This restrictive peaking approximation, when substituted in Eqs. (10), leads directly to the amplitudes[6,9]

$$A_{\mathrm{SPB}}^{\mathrm{FP}}=8(\pi^5 Z_P^3)^{1/2}\left[\left[\frac{Z_P}{2v}\right]^{-2i\nu}\frac{e^{\pi\nu/2}\Gamma(\frac{1}{2}+i\nu)}{\sqrt{\pi}(1+i\nu)}\right]M(0) \tag{12a}$$

and

$$A_{\mathrm{IA}}^{\mathrm{FP}}=8(\pi^5 Z_P^3)^{1/2}M(0)\ . \tag{12b}$$

The fact that $A_{\mathrm{IA}}^{\mathrm{TP}}$ and $A_{\mathrm{IA}}^{\mathrm{FP}}$ are given analytically allows an isolation of that part of the IA amplitude which varies significantly from one approximation to the other and thus to determine which part of the physical mechanism is modeled differently between the two approximations. We pursue this point when discussing the effects of the target bound states.

C. Model potential and cross-section formulas

Section II B dealt with capture from a hydrogenlike target ion. To proceed with inner-shell capture, we introduce, following the discussion of Macek and Alston,[9] the independent-electron model using the scaled Coulomb potential

$$V_S=-Z_S/r+(Z_S^2/2+\epsilon_B)$$

to approximate the exact one-electron K-shell potential. The scaled charge Z_S is defined after Slater[22] and the experimental binding energy ϵ_B for the target K shell is taken from Krause.[23] Modifications of the basic formalism are straightforward as they involve Z_T going to Z_S and the use of the altered relation

$$J^2=K^2+2(\epsilon_B-\epsilon_f)\ ,$$

where

$$K_z=-\tfrac{1}{2}v+(\epsilon_B-\epsilon_f)/v\ .$$

In general, the possibility of capture is greater in the model potential picture since the electron is less tightly bound and moves in a screened Coulomb potential as represented by Z_S.

The total capture cross section for an impact velocity v is obtained by integrating the amplitude squared over all transverse momentum transfers $\vec{K}_\perp$. With azimuthal symmetry we have the integral

$$\sigma=(2\pi v^2)^{-1}\int_0^\infty dK_\perp K_\perp |A(K_\perp)|^2\ , \tag{13}$$

where A is the amplitude. The capture probability $P(b)$, i.e., 2π times the probability that capture takes place for a given impact parameter b and a given velocity v, is simply

$$P(b)=2|a(b)|^2\ , \tag{14}$$

where $a(b)$ is the capture amplitude in the impact parameter representation and the factor of 2 comes from two K-shell electrons. We relate $a(b)$ to $A(K_\perp)$ through the Fourier-Bessel transform after Shakeshaft and Spruch,[24,25]

$$a(b)=(2\pi v)^{-1}\int_0^\infty dK_\perp K_\perp J_0(K_\perp b)A(K_\perp)\ . \tag{15}$$

III. RESULTS AND DISCUSSION

In Sec. III A, we discuss the different weightings of the intermediate states in the SPB and IA theories by presenting ratios of cross sections for capture from a hydrogenlike ion obtained from both full and transverse peaking calculations. Total cross sections and probabilities for K-shell capture are compared with experiment in Sec. III B. Results for the symmetric capture case $Z_P=Z_T=1$ appear in Sec. III C. We first make some comments on the numerical calculations.

In calculating the total cross section or capture probability, the two integrals of Eqs. (11a) and (13) or of Eqs. (11a) and (15) are performed. An adaptive eight-panel Newton-Cotes quadrature routine

was used for both integrations.[26] The individual-panel convergence criterion for the p_z quadrature was taken to be 10^{-2} smaller than the similar criterion for the $K_\perp$ quadrature. This condition helped ensure that the absolute error of the p_z quadrature, that is, of the amplitude itself, was of the order of the desired individual-panel error for the $K_\perp$ quadrature.

The p_z integration around the branch cut was divided into two parts: one along the cut and one along a circle centered at the branch point. Both the large p_z value at which the cut integration is terminated and the radius of the circle are, to some extent, free numerical parameters. In actual calculations, these two parameters as well as the convergence criteria for the two quadratures were all varied independently over several orders of magnitude to establish the overall reliability of the code. This procedure was followed for representative low- and high-velocity cross sections before production runs were executed.

We further checked the code for calculating the transversely peaked SPB amplitude Eq. (11a) by going to large velocities $v \gg Z_T$. In this case the transverse and fully peaked values for the total cross section should converge. Then, since the IA amplitudes are given by analytic expressions and because the off-shell factor should also converge for large v, we have a check of the code. As an example, for $v=100Z_T=1800$, we find the fractional error $|\sigma^{\mathrm{TP}}-\sigma^{\mathrm{FP}}|/\sigma^{\mathrm{FP}}$ to be 0.0202 and 0.0201 for the SPB and IA cross sections, respectively. For a velocity $v=100Z_T$ and target charge of 50, we find the SPB error to be 0.007 27; thus, we have a smaller error (by $\sim\frac{1}{3}$) for a larger target charge (by ~ 3).

The asymptotic cross sections also agree well with the analytic forms derived elsewhere.[6,9] The fully peaked values agree within 1% of the formulas

$$\sigma_{\mathrm{IA}}^{\mathrm{FP}}=\sigma_{\mathrm{BK}}(0.295+5\pi v/2^{11}Z_T)\ (\mathrm{a.u.})$$

and

$$\sigma_{\mathrm{SPB}}^{\mathrm{FP}}=\sigma_{\mathrm{BK}}(0.319+5\pi v/2^{11}Z_T)\ (\mathrm{a.u.})$$

with the asymptotic Brinkmann-Kramers cross section σ_{BK} equal to $2^{18}\pi Z_P^5 Z_T^5/5v^{12}$. The more accurate $\sigma_{\mathrm{IA}}^{\mathrm{TP}}$ agrees well ($\sim 0.6\%$) with the exact IA limit[6]

$$\sigma_{\mathrm{IA}}^{\mathrm{exact}}=\sigma_{\mathrm{BK}}[0.295+5\pi v/2^{11}(Z_P+Z_T)]\ .$$

An analogous SPB result has not been derived due to the difficult integrals involved. Because we do not know the higher-order terms for these asymptotic forms of the cross sections, we can not check the codes for greater accuracy than those listed.

A. Comparison of the IA and SPB theories for capture from a hydrogenlike ion

The total capture cross section is, in general, different when the amplitude is evaluated more accurately. We have given in Eqs. (11) and (12) two sets of amplitudes obtained from two different peaking approximations with the first set being more realistic. The SPB and IA theories are compared by taking ratios of the corresponding cross sections whether they be fully peaked ones or transversely peaked ones. Since the introduction of the model potential basically shifts the cross section upward without changing its form,[9] we compare cross sections for capture from a hydrogenlike target by protons.

Figure 3 presents ratios of SPB and IA cross sections. Recall that the full peaking ratio is a universal function of Z_T/v only. In the velocity region $v \gtrsim Z_T$, we see that the transversely peaked (TP) values converge nicely to the fully peaked (FP) value until very high v where the Thomas peak[5] dominates and the deviations increase again (although their magnitudes are small). This behavior differs markedly from that found in the Jakubassa-Amundsen and Amundsen results[18] where the TP values for $Z_T=10$, 18 are much larger than the FP one until relativistic velocities are reached. The reason for this discrepancy is not known though it may have to do with the approximate evaluation of the off-shell factor in Ref. 18. Our TP values deviate more from the FP value for lower Z_T, that is,

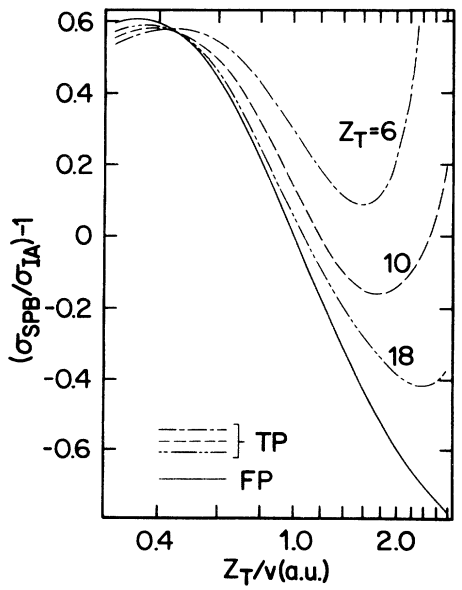

FIG. 3. Ratios of the SPB and IA cross sections for $1s \rightarrow 1s$ capture from hydrogenlike ions by protons with the use of transverse peaking (TP), Eqs. (11), or full peaking (FP), Eqs. (12), for various Z_T.

for lesser asymmetry. Thus when $v \gtrsim Z_T$ the TP values are not greatly different from the FP value although the deviation is a function of the asymmetry.

When $v \lesssim Z_T$ quite a different picture emerges. The SPB cross section at $v \approx Z_T$ is larger than the IA one independent of Z_T. As v decreases, $\sigma_{\rm SPB}^{\rm TP}$ becomes smaller than $\sigma_{\rm IA}^{\rm TP}$ for $Z_T=18$, but the ratio still follows the FP curve. For $Z_T=10$, the same trend is started but quickly reversed and for $Z_T=6$, $\sigma_{\rm SPB}^{\rm TP}$ always remains larger than $\sigma_{\rm IA}^{\rm TP}$. The full peaking approximation seems to break down in the intermediate velocity range and this apparent failure is strongly dependent on the asymmetry. Note that our ratios and those of Ref. 18 agree better for $v \approx Z_T/3$.

The failure of FP is largely confined to the impulse approximation as is apparent from Fig. 4. In this figure we plot the SPB and IA ratios of the TP and FP cross sections as a function of Z_T/v for various Z_T. Except for high velocities, the strong-potential Born TP value is always larger than the FP value. On the other hand, the TP values for the impulse approximation are always smaller than the FP values and the deviations increase as v decreases. For $v \lesssim Z_T$ they are increasingly larger than the SPB deviations which are of the order of 10–15% or even much less as for $Z_T=18$. The large deviations of the IA as shown in Fig. 4 produce in turn the large variations of Fig. 3.

In connection with the increase of the TP cross sections over the FP ones, the SPB theory follows the same trend as in the plane-wave second Born-approximation theory. There, recent exact calculations[27] have shown that approximate evaluations of the amplitude, which also make use of peaking arguments, tend to underestimate the actual amplitude.

Below a velocity roughly around 2.5 a.u., the SPB curve for $Z_T=6$ diverges; this behavior reflects not merely a failure of FP but points to the basic limit of the theory, namely, Z_P^2/v^2 is no longer small. The $Z_T=10$, 18 curves as plotted are still well within the range of validity: for $Z_P^2/v^2=0.1$, the ratio Z_T/v is ~ 3.2 in neon and ~ 5.7 in argon.

The poor modeling of the IA amplitude by the full peaking approximation which is apparent in Figs. 3 and 4 implies that, in the intermediate state momentum integral, the matrix element for excitation to a continuum state is not sufficiently peaked about $\vec{p}=0$. This fact is related to the relative importance of the upper bound states and low continuum of the target to the intermediate-state integral. Consider the amplitudes $A_{\rm IA}^{\rm TP}$ and $A_{\rm IA}^{\rm FP}$ Eqs. (11b) and (12b), respectively, which both contain the factor $\Gamma(1-i\nu)$. Since ν is different in the FP and TP approximations, we also have this factor different in the two approximations. Figure 5 shows a plot of the ratios

$$\sigma_{\rm IA}^{\rm TP}/\sigma_{\rm IA}^{\rm FP}, \quad \left| \frac{\Gamma(1-i\nu_{\rm TP})}{\Gamma(1-i\nu_{\rm FP})} \right|^2,$$

and

$$\frac{[\sigma_{\rm IA}^{\rm TP}/|\Gamma(1-i\nu_{\rm TP})|^2]}{[\sigma_{\rm IA}^{\rm FP}/|\Gamma(1-i\nu_{\rm FP})|^2]}$$

for $Z_T=18$ and where the condition $Z_P^2/v^2 \ll 1$ is always satisfied. We use the IA theory because both $\sigma_{\rm IA}^{\rm TP}$ and $\sigma_{\rm IA}^{\rm FP}$ are given by analytic expressions. It is seen from this figure that the Γ function is the part

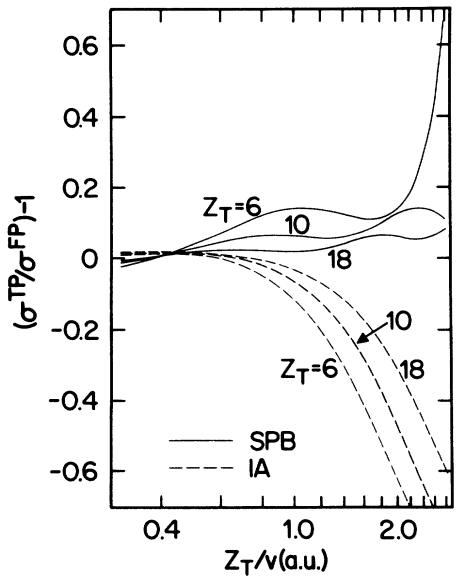

FIG. 4. Ratios of TP and FP cross sections for $1s \rightarrow 1s$ capture from hydrogenlike ions by protons for either the SPB or IA theories for various Z_T.

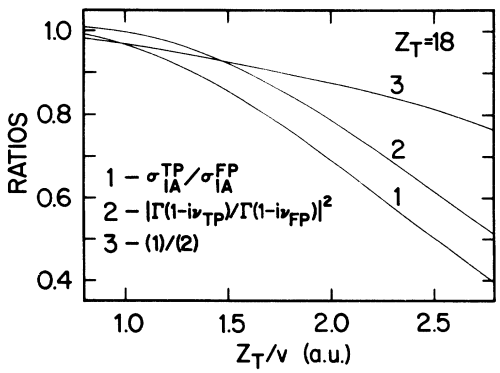

FIG. 5. Ratios of TP and FP values for the IA cross section and components of the cross section for $1s \rightarrow 1s$ capture from Ar^{17+} by protons showing the *relative* variation of these quantities as v decreases.

of the IA amplitude which is modeled poorly in the FP approximation, particularly at low v. On the other hand, the rest of the IA amplitude that gives rise to curve 3 is modeled better.

If we look at the amplitude *before* the p_z integration is done, i.e., at Eqs. (10b), (5), and (7), we see how $\Gamma(1-i\nu)$ as a function of p_z is treated differently in the TP approximation,

$$M(\vec{p})=M(p_z\hat{v}) ,$$

and the FP approximation, $M(\vec{p})=M(0)$. In particular, as we integrate along the negative p_z axis, $\Gamma(1-i\nu)$ changes rapidly in the TP approximation when ϵ is in the lower continuum or is near a bound state. (Recall from Appendix A that the ground state does not appreciably contribute.) For the FP approximation, however, $\Gamma(1-i\nu)$ is smooth for p_z in this region. This difference is accentuated for lower v since the relevant values of p_z are closer to the still-dominant region $p_z\approx 0$. The other factors in $M(p_z\hat{v})$ are not as sensitive to the lower target spectrum and this is reflected again in curve 3. We conclude that the FP approximation does not work well in the IA theory in large part because of the rapid variation of $\Gamma(1-i\nu)$ for p_z near the bound state and lower continuum spectrum of the target.

It is immediately clear why the FP approximation works better in the SPB theory. Comparing IA and SPB amplitudes, Eqs. (10), we see that the off-shell factor of the SPB theory alters the weighting of the various p_z regions. This reweighting is particularly important for the lower intermediate states as pointed out by Macek and Alston. Consider[9] the off-shell factor R defined for the TP approximation as the ratio of p_z integrands of the SPB and IA amplitudes

$$R=\left[\frac{p^2+Z_P^2}{v^2+2vp_z+i\eta}\right]^{-\tau} e^{-i\pi\tau/2}\Gamma(1+\tau)$$

with

$$\tau=i\nu=Z_T/(-v^2-2vp_z-i\eta)^{1/2} .$$

Since $p_z=-v/2$ is the target threshold, we are interested in the region $\vec{p}\approx-\vec{v}/2$. Here, when τ is imaginary (lower continuum), R rapidly oscillates and this behavior compensates for the effects of $\Gamma(1-\tau)$ when integrated over p_z. When τ is real and positive (bound states), we have

$$|R|\approx(2\pi\tau)^{1/2}(p^2\tau/Z_T^2)^{-\tau}e^{-\tau}$$

which is much less than unity, and this compensates, once again, for the effects of $\Gamma(1-\tau)$. For the other regions of p_z, $|R|$ is of order unity and varies more slowly.

We conclude that the IA theory overweights the lower spectrum incorrectly in such a manner as to cause large cancellations in the amplitude. The TP cross section consequently decreases greatly from the FP value. The SPB theory treats the lower spectrum properly with the off-shell factor compensating for the IA overweighting; the overall effect on the cross section is to produce only a relatively small increase of the FP value. Thus, in Fig. 3 the large differences at low v in the $Z_T=6$, 10 TP curves are directly attributable to the different treatments of the threshold region of the target spectrum.

Equations (4a) and (10a) show that a more accurate evaluation of the SPB amplitude than the transverse peaking one involves a change of the relation

$$M(\vec{p})\approx M(p_z\hat{v}) .$$

But from Fig. 5, curve 3, we expect such a change of $M(\vec{p})$ to have a limited effect on the cross section. Moreover, the TP approximation already treats $\Gamma(1-i\nu)$ of $M(\vec{p})$ and the off-shell factor essentially exactly. Thus, the small size of $\vec{p}_\perp\cdot\vec{K}_\perp$ implies that changes in σ in an improved approximation should amount to a few percent or less with a weak velocity dependence.

The extension of the present work to capture into excited states is in certain cases straightforward. Since the momentum wave function $\tilde{\phi}_f(\vec{p})$ is more localized for these states, the neglect of the $\vec{p}_\perp\cdot\vec{K}_\perp$ terms is more well justified. Excited s states and states of higher angular momentum aligned along $\vec{v}$, e.g., $2p$ with $m_l=0$, require no modification of Eq. (11a) other than the replacement of $\tilde{\phi}^*_{1s}(\vec{p})$ by the appropriate $\tilde{\phi}^*_f(\vec{p})$. Such is not the case, however, for the other excited states because the $\vec{p}_\perp$ integral for these automatically gives zero. We must retain the $\vec{p}_\perp\cdot\vec{K}_\perp$ terms to obtain a nonzero amplitude in this situation; the amplitude evaluation will then be more involved, requiring a numerical $p_\perp$ integration in addition to the p_z one.

Since the full peaking amplitude is independent of Z_P/Z_T and the deviations from it are relatively small in the SPB theory, there is the possibility of treating a particular Z_T by a perturbative correction to $\sigma^{\rm FP}_{\rm SPB}$. (The universal FP curve is tabulated in Ref. 9.) Considering Fig. 4, we see that the deviations shown in the SPB curves follow the same *form* as a function of Z_T/v for all three values of Z_T, although the magnitudes are larger for lower Z_T. For example, starting from low Z_T/v the first maximum of the deviation occurs at a Z_T/v value $\frac{2}{3}$ of that for the first minimum for each Z_T. One could reduce the deviation to a function of the quantities Z_P/Z_T and Z_T/v and some constant parameters which would be determined by expanding all factors of the integrand of Eq. (10a) except

$(p_z^2+Z_P^2)^{-1-i\nu}$

in a Taylor series about $p_z=0$; the terms of this series proportional to p_z^2 would determine the constant parameters after p_z integration.

B. Comparison of model potential calculations with experiment

Total cross sections for K-shell capture from carbon, neon, and argon by protons are shown in Figs. 6–8. Theoretical curves were calculated using SPB or IA amplitudes after incorporating a model potential into the formalism in the manner of Sec. II C. Compared to capture from a hydrogenlike ion, the overall effect of the model potential is to increase the cross section. Experimental values are taken from Rødbro *et al.*[28] for carbon, Cocke *et al.*[29] and Rødbro *et al.*[28] for neon, and Macdonald *et al.*,[30] Andriamonje *et al.*,[31] and Horsdal-Pedersen and J. Lahn Rasmussen[32] for argon. The measured values include capture into all final states.

These figures give a striking comparison of the SPB and IA theories. The transverse and full peaking IA cross sections differ greatly at lower velocity, while the transverse and full peaking SPB cross sections differ relatively little ($\lesssim 15\%$). The SPB differences, moreover, are weakly dependent on the charge asymmetry when compared to those of the

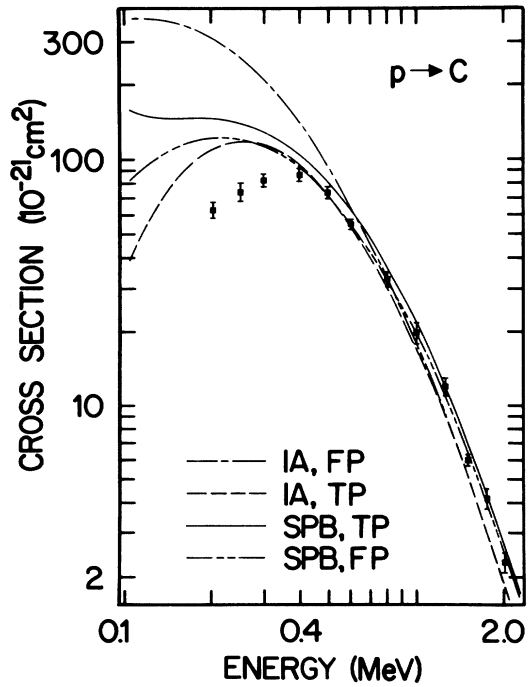

FIG. 6. SPB and IA cross-sections for K-shell capture from carbon by protons. Data are from Rødbro *et al.* (Ref. 28).

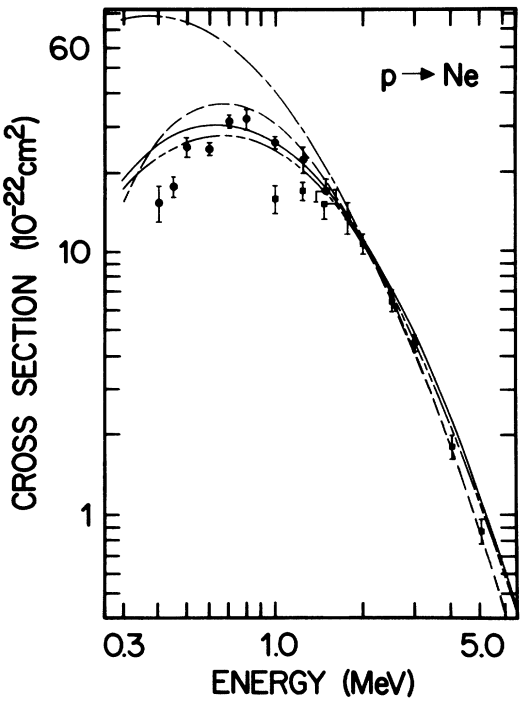

FIG. 7. SPB and IA cross sections for K-shell capture from neon by protons. Data are ●, Rødbro *et al.* (Ref. 28), and ■, Cocke *et al.* (Ref. 29). Curve code is the same as for Fig. 6.

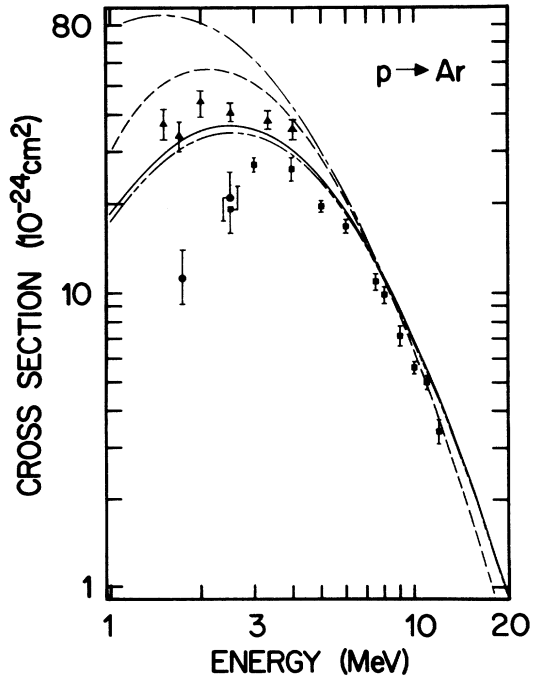

FIG. 8. SPB and IA cross sections for K-shell capture from argon by protons. Data are ▲, Horsdal-Pedersen and Rasmussen (Ref. 32), ●, Andriamonje *et al.* (Ref. 31), and ■, Macdonald *et al.* (Ref. 30). Curve code is the same as for Fig. 6.

IA. Even within the transverse peaking approximation, IA cross sections deviate considerably from SPB ones. As the discussion of Sec. III A has shown, it is the SPB's inclusion of the off-shell factor, which provides for the correct weighting of the intermediate target states, that significantly alters the cross section in comparison with the IA one. This inclusion also allows the simpler full peaking approximation to give a more realistic treatment of the capture process in the SPB theory. The latter result is a desirable feature because of the approximate charge scaling known to exist for inner-shell capture.[28]

The SPB cross sections give generally good agreement with the experimental data, considering the theory does not include capture into excited states. The agreement is better than for the IA values which are seen to be too large for velocities below the matching velocity $v=Z_S$. The matching velocity corresponds to incident energies of ~ 0.8 MeV for carbon, ~ 2.4 MeV for neon, and ~ 7.8 MeV for argon. At low incident energies, e.g., around ~ 0.4 MeV in neon, the SPB values are above the data. This most probably points to the limitation of the theory, since $(Z_P/v)^2$ is not extremely small then. For carbon near an energy of 0.1 MeV, $\sigma_{\rm SPB}^{\rm TP}$ diverges from $\sigma_{\rm SPB}^{\rm FP}$ for the same reason. A possible reason for the SPB values being too large at large velocity will be mentioned shortly.

The discrepancy between the two sets of data points in neon[28,29] and argon[30,32] is a result of the larger values being measured by taking better account of the small impact-parameter contributions to the cross section.

Figures 9–11 present capture probabilities $P(b)$ following Eqs. (14) and (15) for protons on neon and argon. The strong-potential Born TP probabilities are always larger than the corresponding FP ones; the reverse is true of the impulse approximation. Moreover, the ratios of the two sets of values are relatively independent of the impact parameter. For example, with 0.7-MeV protons incident on neon we have the ratios

$$P_{\rm SPB}^{\rm TP}/P_{\rm SPB}^{\rm FP}=1.09$$

and

$$P_{\rm IA}^{\rm TP}/P_{\rm IA}^{\rm FP}=0.61$$

for $b=0.3a_0/Z_S$ changing monotonically to 1.10 and 0.59, respectively, for $b=2.6a_0/Z_S$. Here, a_0 is the Bohr radius and $Z_S=Z_T-0.3$. The same behavior holds generally for all the probabilities. These ratios are exactly what one reads from the total cross-section curves; that is, on Fig. 7 we find

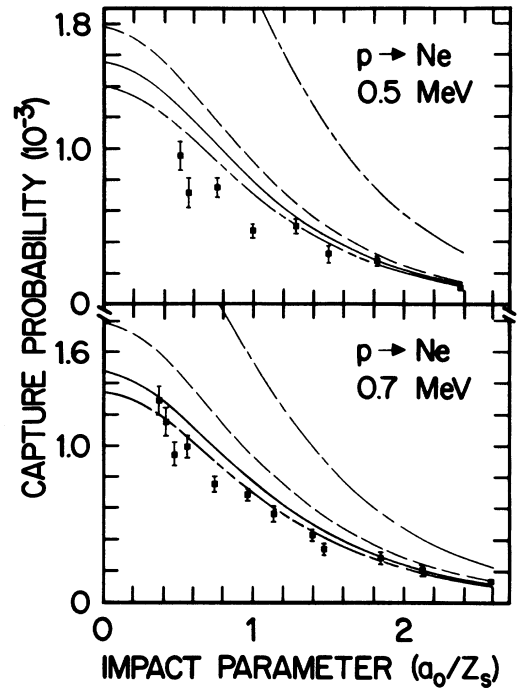

FIG. 9. SPB and IA probabilities for K-shell capture from neon by protons. Data are from Horsdal-Pedersen (Ref. 33). Curve code is as in Fig. 6.

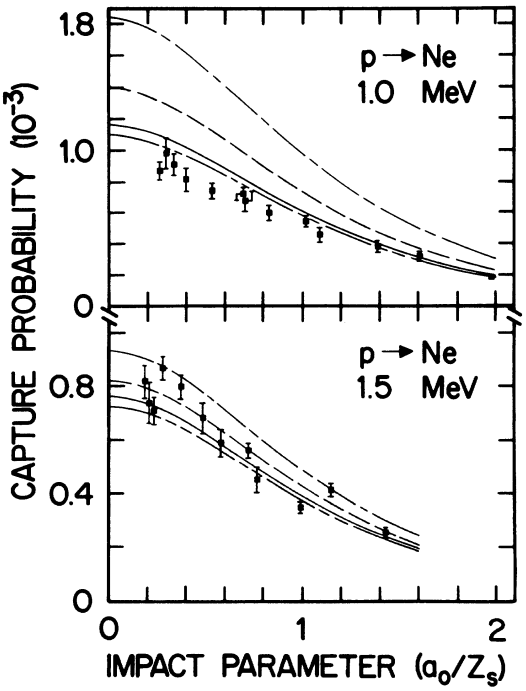

FIG. 10. SPB and IA probabilities for K-shell capture from neon by protons. Data are from Horsdal-Pedersen (Ref. 33). Curve code is as in Fig. 6.

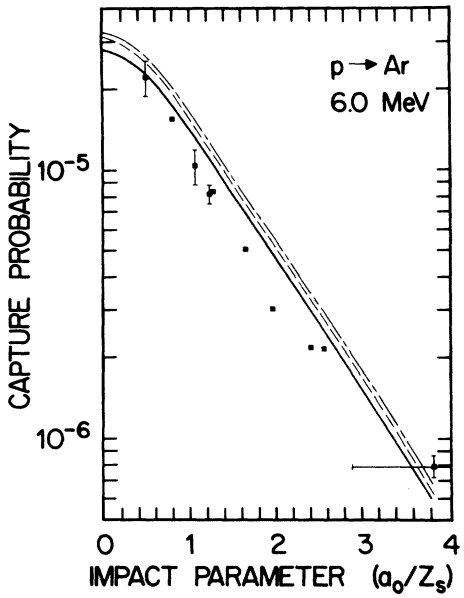

FIG. 11. SPB and IA probabilities for K-shell capture from argon by protons. Data are from Cocke *et al.* (Ref. 34). Curve code is as in Fig. 6.

$$\sigma_{\mathrm{SPB}}^{\mathrm{TP}}/\sigma_{\mathrm{SPB}}^{\mathrm{FP}}=1.09$$

at 0.7 MeV and

$$\sigma_{\mathrm{IA}}^{\mathrm{TP}}/\sigma_{\mathrm{IA}}^{\mathrm{FP}}=0.61$$

at the same energy. Thus, there is no major redistribution of the amplitude versus b in an improved approximation, as may be expected since the off-shell factor does not depend on $K_\perp$.

The agreement of the SPB probabilities with the experimental data of Horsdal-Pedersen[33] for neon and of Cocke *et al.*[34] for argon is better than for the IA ones, although the TP values in some cases improve agreement and in other cases lessen agreement. Since the argon data and calculations are at higher energy, the SPB and IA results do not differ greatly. Notice also the linear character of the argon curves implying a decreasing exponential behavior for $P(b)$ and therefore $|a(b)|$. This behavior follows from the character of the Fourier-Bessel transform of $a(b)$ and from the sizes of b and $K_\perp$; it reflects the exponential nature of the initial charge distribution.

One possible reason for the discrepancy with experiment is that our $P(b)$ does not take into account the competing process in which an L-shell electron is captured by the projectile at the same time a K-shell electron is excited to fill the L shell. This process is experimentally indistinguishable from the supposed dominant process considered in this paper. But in the region $v \gtrsim Z_T$, the K-shell capture probability $P_K(b)$ (we attach the subscript for clarity) is extremely small; for example, in argon for K-shell capture by 7-MeV protons, we have $P_K(b)\approx 10^{-5}$ or

$$|a_K(b)| \approx 0.003 .$$

Since the two processes are coherent (they have the same final state), we must add amplitudes. Jakubassa-Amundsen[35] has calculated argon L-shell capture probabilities $P_L(b)$. She finds

$$P_L(b)\approx 2\times 10^{-4}$$

for 1-MeV protons in the impact-parameter range of interest here. It may be expected that at 6 MeV $P_L(b)\approx 10^{-4}$. For a $1s\rightarrow 2s$ excitation[36] probability $P_X(b)$ of the order of 10^{-3}, the capture probability for the two-step mechanism is of the order $P_X P_L \approx 10^{-7}$, corresponding to an amplitude of the order of 0.3×10^{-3}. This represents a 10% contribution to the overall capture amplitude which could raise *or* lower the resulting probability.

C. Symmetric capture

For symmetric collisions, the effects of a more accurate treatment of the target spectrum on the capture cross section have been discussed by Macek and Alston.[9] They show, using the full peaking approximation, that the SPB $1s\rightarrow 1s$ total cross section for protons on hydrogen lies below the Brinkman Kramers[2] (BK) cross section in the range of impact energies (in MeV)

$$0.1 \lesssim E \lesssim 10.0 .$$

This result contrasts with the behavior of the exact second-order BK (BK2) cross section[37] which lies above the BK one for E from 0.1 to ~ 3 MeV. It is known, however, that the BK theory already overestimates the capture probability; thus, for the lower energies, we attribute the difference in behavior of the SPB and BK2 cross sections to a poor representation of the intermediate target spectrum in the BK2 theory. That is, the lack of discrete target states and the use of plane waves for the continuum states in the BK2 theory lead to an unphysical increase in the cross section.

While the approximation of going to the energy shell, Eq. (4a), is well justified for the symmetric case, the further approximation of full peaking is not so clearly justified. It is of some interest, then, to see whether the transversely peaked values of the SPB cross section also lie below the BK one. Table I gives BK, BK2, and SPB cross sections in πa_0^2 over a broad energy range. (Since the TP values are presumably more accurate, the FP values are not

TABLE I. Cross sections for $1s \rightarrow 1s$ captures when $Z_P = Z_T = 1$. The BK and second-order BK (BK2) values are from McGuire (Ref. 37) except for the BK2 values at 0.1 and 0.2 MeV which are from Wadehra *et al.* (Ref. 27). The SPB values were obtained using Eq. (11a). The number in parentheses is the power of 10 multiplying the corresponding table entry [e.g., 3.28(−4) denotes 3.28×10^{-4}].

E (MeV)	σ_{BK} (πa_0^2)	σ_{BK2} (πa_0^2)	σ_{SPB} (πa_0^2)
0.1	0.398	1.4	0.542
0.2	0.0262	0.074	0.0214
0.5	3.28(−4)	7.95(−4)	1.74(−4)
1.0	7.91(−6)	13.63(−6)	3.52(−6)
5.0	7.38(−10)	6.09(−10)	3.09(−10)
10.0	12.11(−12)	8.04(−12)	5.57(−12)
50.0	8.07(−16)	4.51(−16)	6.80(−16)

given; in general, the TP values are greater than the FP ones.) We see that, except for the very lowest energy, the SPB values remain below the BK ones. At 0.1 MeV the applicability of the theory is questionable since this corresponds to a velocity of ~ 2 a.u. The coupled-states calculation of Shakeshaft[38] gives 0.0053 πa_0^2 for the cross section at 0.2 MeV so that the SPB value is a factor of 4 too high, although it agrees much better than does the BK2 estimate.

The SPB cross sections were obtained from Eq. (11a) with the following modifications. The minimum momentum transfer K_z is set equal to its exact value of $-\frac{1}{2}v$. For $1s \rightarrow 1s$ capture, the relation

$$J^2 + 2\epsilon_f = K^2 + 2\epsilon_i$$

reduces to $J^2 = K^2$.

At asymptotically high velocities, both the BK2 and SPB cross sections are known[5,9] to have a velocity dependence of v^{-11} as compared to the v^{-12} dependence of the BK cross section. Table I shows that this behavior has not yet allowed the second-order theories to dominate the first-order one at the very high energy of 50 MeV, but the SPB cross section appears close to doing so. The impact velocity is $\sim 0.3\ c$ for 50 MeV—a velocity for which relativistic effects could be important.

IV. CONCLUSION

We have established that the correct treatment of the lower target spectrum in the SPB theory is an important factor allowing the full peaking approximation to represent the exact amplitude with moderate accuracy.

We have also shown that the correct treatment of the target spectrum produces major changes in the capture cross section itself as compared to the IA one. The structure of the SPB amplitude has been clarified in this study and the theory is shown to be soundly based and internally consistent; moreover, the approximation is seen to give a good representation of the measured cross sections.

ACKNOWLEDGMENTS

I gratefully acknowledge the advice and continual guidance of Professor Joseph Macek to whom this work owes much. His assistance with the manuscript is also greatly appreciated. I also want to thank Professor Erik Horsdal-Pedersen for the use of his data before publication. This work was supported by the National Science Foundation under Grant No. PHY-81-07147.

APPENDIX A: CONTRIBUTIONS TO THE AMPLITUDE FROM THE REGION $\vec{p} \approx \vec{K}$

While the region $p \lesssim Z_P$ does indeed give the dominant contributions to the amplitude, one notes that $\tilde{V}_{Pe}(\vec{p} - \vec{K})$ peaks for large $\vec{p} \approx \vec{K}$. For completeness we show this region gives a negligible contribution. We do this by integrating over the finite volume of order Z_P^3 centered at $\vec{p} = \vec{K}$. The value obtained is compared with the rough estimate[39] of the fully peaked value of the amplitude which is $(Z_P Z_T)^{5/2}/K^6$. The limited integration volume is justified since the integrand is peaked and because $\tilde{\phi}_f^*(\vec{p})$ dominates $\tilde{V}_{Pe}(\vec{p} - \vec{K})$ at large distances from $\vec{p} = \vec{K}$.

Our starting point is the amplitude given by Eq. (2.17) of Macek and Alston[9] in which the matrix element involving the off-shell wave function has been reduced to a one-dimensional parametric integral. Their result is

$$A_{SPB} = (2\pi)^{3/2} \int d^3p\, \tilde{\phi}_f^*(\vec{p}) \tilde{V}_{Pe}(\vec{p} - \vec{K}) [M_1(\vec{p}) + M_2(\vec{p})] , \tag{A1}$$

where

$$M_1(\vec{p}) = \langle \phi_{\vec{p} + \vec{v}}(\vec{r}) \,|\, e^{i(\vec{p} - \vec{K}) \cdot \vec{r}} \,|\, \phi_i(\vec{r}) \rangle \tag{A2}$$

and

$$M_2(\vec{p})=\frac{16\pi Z_T N_i X}{(2\pi)^{3/2}(1-e^{-2\pi i\tau})}\frac{\partial}{\partial\mu_1}\int_C d\rho\,\rho^{-\tau}\{D_1D_2-2[E_1E_2+4X^2\vec{k}_1\cdot\vec{k}_2]\rho+F_1D_2\rho^2\}^{-1}\,. \tag{A3}$$

The contour C starts at $1+i0$, encircles the origin within the unit circle, and ends at $1-i0$. The other quantities are defined by the relations

$$X=[-2(\epsilon+i\eta)]^{1/2},\ \mathrm{Re}X>0;\ \tau=Z_T/X;\ D_i=(X+\mu_i)^2+k_i^2\,;$$

$$E_i=X^2-\mu_i^2-k_i^2;\ F_1=(X-\mu_1)^2+k_i^2;\ \phi_i(\vec{r})=N_ie^{-\mu_1 r},\ N_i=(Z_T^3/\pi)^{1/2}\,,$$

where $\vec{k}_1=\vec{p}-\vec{K}$, $\vec{k}_2=\vec{p}+\vec{v}$, and $\mu_2=0$. After the μ_1 differentiation in Eq. (A3), we set μ_1 equal to Z_T. Equation (A1) is still an exact expression. We now proceed to evaluate it for the region $\vec{p}\approx\vec{K}$.

Define the vector $\vec{\delta}\equiv\vec{p}-\vec{K}$ with $\delta\lesssim Z_P\ll Z_T$, assume a $1s$ final state, and suppress numerical coefficients; our amplitude Eq. (A1) becomes

$$A_{\mathrm{SPB}}\propto Z_P^{5/2}\int d^3\delta[(\vec{K}+\vec{\delta})^2+Z_P^2]^{-2}(\delta^2+\alpha^2)^{-1}[M_1+M_2(\vec{K}+\vec{\delta})]\,, \tag{A4}$$

where

$$M_1\propto Z_T^{5/2}(K^2+Z_P^2)^{-2} \tag{A5}$$

and

$$M_2\propto\frac{Z_T^{5/2}X}{1-e^{-2\pi i\tau}}\frac{\partial}{\partial\mu_1}\int_C d\rho\,\rho^{-\tau}\{D_1D_2-2[E_1E_2+4X^2\vec{\delta}\cdot(\vec{\delta}-\vec{J})]\rho+F_1D_2\rho^2\}^{-1}\,. \tag{A6}$$

We have used the relation $K^2+2\epsilon_i=J^2+2\epsilon_f$ to gain Eq. (A5). In Eq. (A4), $\alpha\to 0_+$ is a convergence factor.

Recalling that $\mu_1=Z_T$ and $K_z\equiv-\frac{1}{2}v-(\epsilon_f-\epsilon_i)/v$, we have the order-of-magnitude estimates

$$|F_1/D_1|\approx\delta^2/Z_T^2\ll 1\,,$$

$$|[E_1E_2+4X^2\vec{\delta}\cdot(\vec{\delta}-\vec{J})]/D_1D_2|\approx|K^2\vec{v}+2Z_T^2\vec{K}|\,\delta/K^2Z_T^2\ll 1\,,$$

where we have expanded D_1, D_2, etc., in powers of $\vec{\delta}$. These small ratios together with $|\rho|<1$ allow us to evaluate the ρ integral by keeping only the factor $\rho^{-\tau}$. Using the approximate forms

$$X\approx Z_T-v\delta_z/Z_T-i\eta,\ \ \tau\approx 1+v\delta_z/Z_T^2+i\eta\,, \tag{A7}$$

we find

$$(1-e^{-2\pi i\tau})^{-1}\int_C d\rho\cdots\approx\left[\frac{Z_T^2}{v(\delta_z+i\eta)}+O(\delta)\right]\frac{1}{D_2}\frac{\partial}{\partial\mu_1}\frac{1}{D_1}\bigg|_{\mu_1=Z_T}\,. \tag{A8}$$

Substituting Eqs. (A7) and (A8) into our expression for M_2 [Eq. (A6)] and retaining only terms linear in $\vec{\delta}$, we obtain

$$M_2(\vec{K}+\vec{\delta})\propto -Z_T^{5/2}\frac{(1+v\delta_z/2Z_T^2-2\vec{K}\cdot\vec{\delta}/K^2)}{vK^2(\delta_z+i\eta)}\,. \tag{A9}$$

If we insert Eq. (A9) and the expression for M_1 [Eq. (A5)] into the SPB amplitude Eq. (A4), the large $\vec{p}$ contributions are seen to be

$$A_{\mathrm{SPB}}(\vec{p}\approx\vec{K})\propto\left[\frac{(Z_PZ_T)^{5/2}}{K^6}\right]\times\left[\frac{Z_P}{K^2}-B\left[\frac{Z_P}{2Z_T^2}-\frac{6Z_PK_z}{vK^2}\right]\right],$$

where B is some number of the order of unity.

The term Z_P/K^2 in the second set of brackets is from M_1 and is the relative contribution of the first Born term. The second two terms are the relative contribution of the second Born term. This result shows the contributions to the amplitude from the large $\vec{p}\approx\vec{K}$ region are smaller by factors of the order $(Z_P/v)^2$ or $(Z_P/Z_T)^2$ and confirms the well-known observation[40] that, in second-order theories, large momentum components of the final bound state do not appreciably contribute to capture. However, the SPB theory contains the target bound states in the intermediate-state integral and this fact somewhat restricts the definition of large momentum components which give rise to negligible contributions.

The bound-state poles are located at

$$p_z = -\tfrac{1}{2}v - (\epsilon_f + Z_T^2/2n^2)/v - i\eta$$

and, in particular, the ground-state pole is at $p_z = K_z - i\eta$ corresponding to $\delta_z = 0$. For $\delta_z \approx 0$, the estimate Eq. (A7) holds and thus the ground state does not contribute significantly as an intermediate state. The same is not true, though, of the excited states and especially the highly excited ones, since in this case δ is of the order $Z_T^2/2v$ and not small. The poles corresponding to these states are close to the origin $\vec{p} = 0$ and are expected to contribute significantly when $\epsilon \approx 0$, as suggested by Fig. 1.

APPENDIX B: DISCUSSION OF THE SINGULARITY STRUCTURE OF THE INTEGRAND IN THE AMPLITUDE

Considering the various factors of the integrand in the amplitude Eq. (10a), we observe that the bound-state poles

$$p_z \approx -\tfrac{1}{2}(v + Z_T^2/n^2 v) - i\eta$$

arising from the factor $\Gamma(1 - i\nu)$ of $M(p_z \hat{v})$ and the branch point

$$p_z = \{[K(v - iZ_T)/2vK_z]^2 - 1\}v$$

arising from the term

$$[(\mu - iv)^2 + K^2 - 2p_z(K_z + v + i\mu)]^{-i\nu}|_{\mu = Z_T}$$

are located in the *lower* half-plane.

There are also poles at $p_z = K_z \pm K_\perp$. The residue of the one in the upper half-plane contributes to the amplitude. In general, the form of the integrand given in Eq. (10a) does not represent the exact integrand well when $\vec{p}$ is large because terms of order $(p/v)^2$ have been neglected; however, because K_z is large and the contributions correspond to the $\vec{p} \approx \vec{K}$ region, we do not include them here. Finally, of the remaining two branch points at $p_z = \pm iZ_P$, only one is in the upper half-plane. We further note that the bound-state poles are arbitrarily near to the $-p_z$ axis and therefore complicate a numerical integration along this axis, but for the cut integration, all the singular points except those at $\pm iZ_P$ are located at distances of the order v or Z_T from the origin of p_z integration for all K. The conditions $Z_P/v \ll 1$ and $Z_P/Z_T \ll 1$ imply the corresponding factors of the integrand vary slowly in the region $p_z \approx iZ_P$.

Therefore, we conclude that, from a numerical point of view, integration around the cut is clearly the best way to evaluate the SPB amplitude.

The cuts for the branch points besides those at $\pm iZ_P$ must be compatible with the phase convention

$$\pi < \arg(-Z) \leq +\pi$$

with Z equal to

$$\Delta[K^2 + (Z_T - iv)^2 - 2p_z(K_z + v + iZ_T)] ,$$

where Δ is defined in Eq. (6). This condition follows[41] from the derivation of Eq. (4a). We have chosen the cuts for the factors of

$$(p_z^2 + Z_P^2)^{-1-i\nu}$$

so that the respective branches are defined as

$$|p_z + iZ_P| > 0, \quad -\pi/2 \leq \arg(p_z + iZ_P) < +3\pi/2$$

and

$$|p_z - iZ_P| > 0, \quad -3\pi/2 < \arg(p_z - iZ_P) \leq +\pi/2 .$$

Our discussion of the integrand of the SPB amplitude Eq. (10a) given here can be applied to the integrand of the IA amplitude Eq. (10b). The only difference is that we have poles at $p_z = \pm iZ_P$.

[1] J. R. Oppenheimer, Phys. Rev. 31, 349 (1928).
[2] H. C. Brinkman and H. A. Kramers, Proc. Acad. Sci. Amsterdam 33, 973 (1930).
[3] Wm. Lichten, Phys. Rev. 131, A1025 (1965).
[4] D. R. Bates, Proc. R. Soc. London, Ser. A 724, 294 (1958); C. D. Lin, S. C. Soong, and L. N. Tunnell, Phys. Rev. A 17, 1646 (1978).
[5] L. H. Thomas, Proc. R. Soc. London 114, 561 (1927); R. M. Drisko, Ph.D. thesis, Carnegie Institute of Technology, 1955 (unpublished).
[6] J. S. Briggs, J. Phys. B 10, 3075 (1977).
[7] J. H. Macek and R. Shakeshaft, Phys. Rev. A 22, 1441 (1980).
[8] J. Macek and K. Taulbjerg, Phys. Rev. Lett. 46, 170 (1981).
[9] J. Macek and S. Alston, Phys. Rev. A 26, 250 (1982).
[10] D. H. Jakubassa-Amundsen and P. A. Amundsen, Z. Phys. A 297, 203 (1980).
[11] L. Dubé and J. Briggs, J. Phys. B 14, 4595 (1981).
[12] See p. 314 of Dž. Belkić, R. Gayet, and A. Salin, Phys. Rep. 56, 279 (1979).
[13] J. Eichler and F. T. Chan, Phys. Rev. A 20, 104 (1979).

[14]R. Shakeshaft, Phys. Rev. A 17, 1011 (1978).
[15]For a more in depth comparison of the second—Born-approximation—type theories see J. S. Briggs, J. H. Macek, and K. Taulbjerg, Comments At. Mol. Phys. 12, 1 (1982).
[16]P. A. Amundsen and D. H. Jakubassa, J. Phys. B 13, L467 (1980).
[17]L. Kocbach, J. Phys. B 13, L665 (1980).
[18]D. H. Jakubassa-Amundsen and P. A. Amundsen, J. Phys. B 14, L705 (1981).
[19]See the footnote on p. 539 of the paper by J. D. Jackson and H. Schiff, Phys. Rev. 89, 359 (1953).
[20]E. J. Kelsey and J. Macek, J. Math. Phys. 17, 1182 (1976).
[21]R. A. Mapleton, J. Math. Phys. 2, 482 (1961).
[22]J. C. Slater, Phys. Rev. 36, 57 (1930).
[23]M. O. Krause, Oak Ridge National Laboratory Report No. ORNL-TM-2943, 1970 (unpublished).
[24]R. McCarroll and A. Salin, J. Phys. B 1, 163 (1968).
[25]L. Wilets and S. J. Wallace, Phys. Rev. 169, 84 (1968).
[26]G. E. Forsythe, M. A. Malcolm, and C. B. Moler, *Computer Methods for Mathematical Computations* (Prentice-Hall, Englewood Cliffs, 1977), Ch. 5.
[27]J. M. Wadehra, R. Shakeshaft, and J. H. Macek, J. Phys. B 14, L767 (1981); P. R. Simony and J. H. McGuire, in Proceedings of the Seventh International Conference on Atomic Physics, MIT, 1980 (unpublished); J. E. Maraglia, R. D. Piacentini, R. D. Rivarola, and A. Salin, J. Phys. B 14, L197 (1981); see also P. J. Kramer, Phys. Rev. A 6, 2125 (1972).
[28]M. Rødbro, E. Horsdal-Pedersen, C. L. Cocke, and J. R. Macdonald, Phys. Rev. A 19, 1936 (1979).
[29]C. L. Cocke, R. K. Gardner, B. Curnutte, T. Bratton, and T. K. Saylor, Phys. Rev. A 16, 2248 (1977).
[30]J. R. Macdonald, C. L. Cocke, and W. W. Eidson, Phys. Rev. Lett. 32, 648 (1974).
[31]S. Andriamonje, J. F. Chemin, J. Routurier, J. N. Scheurer, H. Laurent, and J. P. Schapira, in *Abstracts of the Proceedings of the Twelfth International Conference on the Physics of Electronic and Atomic Collisions, Gatlinburg, 1981,* edited by S. Datz (North-Holland, Amsterdam, 1981), p. 657.
[32]E. Horsdal-Pedersen and J. Lahn Rasmussen, private communication.
[33]E. Horsdal-Pedersen, in *Proceedings of the Twelfth International Conference on the Physics of Electronic and Atomic Collisions, Gatlinburg, 1981,* Ref. 31, p. 139.
[34]C. L. Cocke, J. R. Macdonald, B. Curnutte, S. L. Varghese, and R. Randall, Phys. Rev. Lett. 36, 782 (1976). The cross sections used from this reference are differential in angle. I have converted them to $P(b)$ by means of the relation

$$P(b)=\left[\frac{d\sigma}{d\Omega}\right]_{\text{capture}}\Big/\left[\frac{d\sigma}{d\Omega}\right]_{\text{elastic}}$$

with

$$\left[\frac{d\sigma}{d\Omega}\right]_{\text{elastic}}=\left[\frac{Z_P Z_{\text{eff}}}{4E\sin^2(\theta/2)}\right]^2 \approx\left[\frac{Z_P Z_{\text{eff}}}{E\theta^2}\right]^2$$

and

$$b(\theta)=\frac{Z_P Z_{\text{eff}}}{2E}\cot\left[\frac{\theta}{2}\right] \approx\frac{Z_P Z_{\text{eff}}}{E\theta}\,.$$

For the small impact parameters relevant here, we use

$$Z_{\text{eff}}=(-2\epsilon_B)^{1/2}$$

for the K shell. See V. Dose, Helv. Phys. Acta 41, 261 (1968).
[35]D. H. Jakubassa-Amundsen, J. Phys. B 14, 2647 (1981).
[36]J. S. Briggs, Rep. Prog. Phys. 39, 217 (1976).
[37]J. McGuire, private communication.
[38]R. Shakeshaft, Phys. Rev. A 18, 1930 (1978).
[39]See Eqs. (5.1) and (5.4) of Ref. 9.
[40]R. Shakeshaft and L. Spruch, Rev. Mod. Phys. 51, 369 (1979).
[41]See after Eq. (4.14) of Ref. 9.